0026-895X/09/7602-290–300$20.00
MOLECULAR PHARMACOLOGY
Copyright © 2009 The American Society for Pharmacology and Experimental Therapeutics
Mol Pharmacol 76:290–300, 2009

Vol. 76, No. 2
55418/3496927
Printed in U.S.A.

Antitumor Effects of Dehydroxymethylepoxyquinomicin, a Novel Nuclear Factor-κB Inhibitor, in Human Liver Cancer Cells Are Mediated through a Reactive Oxygen Species-Dependent Mechanism

Nadia Lampiasi, Antonina Azzolina, Natale D'Alessandro, Kazuo Umezawa, James A. McCubrey, Giuseppe Montalto, and Melchiorre Cervello

Institute of Biomedicine and Molecular Immunology "Alberto Monroy," National Research Council, Palermo, Italy (N.L., A.A., M.C.); Departments of Pharmacological Science (N.D.) and Clinical Medicine & Emerging Pathologies (G.M.), University of Palermo, Palermo, Italy; Department of Applied Chemistry, Faculty of Science and Technology, Keio University, Yokohama, Japan. (K.U.); and Department of Microbiology and Immunology, Brody School of Medicine at East Carolina University, Greenville North Carolina (J.A.M.)

Received February 16, 2009; accepted May 20, 2009

ABSTRACT

Activation of the nuclear transcription factor-κB (NF-κB) has been implicated in liver tumorigenesis. We evaluated the effects of a novel NF-κB inhibitor, dehydroxymethylepoxyquinomicin (DHMEQ), in two human liver cancer cell lines HA22T/VGH and HuH-6. DHMEQ treatment dose dependently decreased the DNA-binding capacity of the NF-κB p65 subunit, inhibited cell growth and proliferation, and increased apoptosis as shown by caspase activation, release of cytochrome *c*, poly(ADP-ribose) polymerase cleavage, and down-regulation of survivin. DHMEQ also induced a dose-dependent activation of mitogen-activated protein kinase kinase/extracellular signal-regulated kinase signaling, and inhibition of this pathway significantly reduced cell growth. It is noteworthy that we observed that DHMEQ stimulated reactive oxygen species (ROS) production in a dose-dependent manner and that pretreatment of the cells with the antioxidant *N*-acetyl-L-cysteine (NAC) significantly reduced DHMEQ-induced ROS generation. Accordingly, NAC completely reversed the DHMEQ-induced growth inhibition, caspase activation, and cell death. DHMEQ-treated cells exhibited DNA damage, as evaluated by accumulation in nuclear foci of phospho-H2AX, which was completely reversed by NAC. Moreover, DHMEQ induced the expression of genes involved in the endoplasmic reticulum stress response (*GRP78*, *CHOP*, *TRB3*) and promoted the splicing of XBP1 mRNA in a dose-dependent fashion in both cell lines, which was reversed in the presence of NAC. Knockdown of TRB3 mRNA expression by small interference RNA significantly decreased DHMEQ-induced cell growth inhibition. These data suggest that DHMEQ antitumor effects are primarily mediated through ROS generation. Thereby, considering that cancer cells are under increased ER stress and oxidative stress conditions, DHMEQ may greatly improve various anticancer strategies.

Hepatocellular carcinoma (HCC) is one of the most common malignancies worldwide. Several strategies have been attempted to improve the treatment of patients with HCC; unfortunately, it is a tumor type with a high lethality. Therefore, novel approaches are required to successfully treat this cancer.

Cancer cells are under oxidative stress associated with increased metabolic activity and production of reactive oxygen species (ROS) (Szatrowski and Nathan, 1991). In contrast, in normal cells, ROS are produced at low concentra-

This work was supported by the Associazione Italiana per la Ricerca sul Cancro (AIRC) and the Italian National Research Council (CNR) [Istituto di Biomedicina e Immunologia Molecolare]

Article, publication date, and citation information can be found at http://molpharm.aspetjournals.org.

doi:10.1124/mol.109.055418.

ABBREVIATIONS: HCC, hepatocellular carcinoma; ROS, reactive oxygen species; ERK, extracellular signal-regulated kinase; ER, endoplasmic reticulum; MEK, mitogen-activated protein kinase/extracellular signal-regulated kinase; GRP78, glucose-regulated protein 78; CHOP, CAAT/enhancer-binding protein homologous transcription factor; TRB3, tribbles homolog 3; NF-κB, nuclear factor-κB; DHMEQ, dehydroxymethylepoxyquinomicin; NAC, *N*-acetyl-L-cysteine; FBS, fetal bovine serum; BAPTA, 1,2-bis(2-aminophenoxy)ethane-*N*,*N*,*N*′,*N*′-tetraacetic acid; AM, acetoxymethyl ester; TTFA, thenoyltrifluoroacetone; DPI, diphenyleneiodonium; U0126, 1,4-diamino-2,3-dicyano-1,4-bis(methylthio)butadiene; BrdU, 5-bromo-2′-deoxyuridine; PARP, poly(ADP-ribose) polymerase; RT-PCR, reverse transcription-polymerase chain reaction; H_2DCFDA, 2′,7′-difluorodihydrofluorescein diacetate; PBS, phosphate-buffered saline; MTS, 3-(4,5-dimethylthiazol-2-yl)-5-(3-carboxymethoxyphenyl)-2-(4-sulfophenyl)-2*H*-tetrazolium; MRC, mitochondrial respiratory chain; XBP1, X-box binding protein 1.

tions and are effectively neutralized by the potent antioxidant system of the cells. ROS can be produced intracellularly from mitochondrial respiratory chain complexes (Richter and Schweizer, 1997), from the radical-generating enzymes xanthine/xanthine oxidase (McCord, 1985), and from plasma membrane NADPH, oxidases (Trudel et al., 1991). Phospholipase A_2-activated arachidonic acid metabolism can also be a source of ROS (Henderson et al., 1989). Although increased ROS production plays an important role in maintaining cancer phenotype because of their stimulating effects on cell growth, proliferation, and genomic instability through DNA damage, excessive levels of ROS beyond the antioxidant capacity of the cells can induce cell cycle arrest and apoptosis. Therefore, drugs that modulate the production of ROS have been proposed as therapeutic strategies to selectively target the destruction of cancer cells. ROS-stressing agents can effectively kill cancer cells because cells become sensitive beyond a threshold (Cabello et al., 2007). ROS-induced apoptosis implies either a direct toxic effect as well as a function of ROS as signaling molecules that trigger the activation of pro-death pathways (Ueda et al., 2002).

One of the major pathways through which apoptosis is induced is the stress- or mitochondria-mediated caspase-9 activation pathway. Oxidative stress induces cytochrome *c* release from mitochondria and activation of caspases and protein kinases (Ueda et al., 2002). Recent studies have shown that ROS can activate mitogen-activated protein kinases, including the extracellular signal-regulated kinases-1/2 (ERK1/2) (Gupta et al., 1999). These kinases are involved in cell proliferation, differentiation, and apoptosis. In addition, the mitogen-activated protein kinase/ERK (MEK)/ERK pathway contributes to maintain cell survival during oxidative stress (Kuznetsov et al., 2008).

Accumulating evidence suggests that, in addition to mitochondria, the endoplasmic reticulum (ER) is also an important apoptotic control point (Danial and Korsmeyer, 2004). In fact, accumulation of unfolded protein in the ER induces the ER stress response, otherwise known as the unfolded protein response. Cells initially adapt to the accumulation of unfolded proteins by inducing the expression of ER-resident molecular chaperones such as the Ca^{2+}-binding glucose-regulated protein 78 (GRP78) (Li and Lee, 2006). Moreover, one of the ER protein sensors, inositol-requiring ER-to-nucleus signal kinase 1, has an endoribonuclease activity that removes 26 nucleotides from X-box binding protein 1 (XBP1) mRNA, thus resulting in a new transcription factor that induces expression of chaperone genes (Lee et al., 2003). However, if adaptation is not sufficient, the apoptotic response is initiated, which is primarily the induction of CAAT/enhancer-binding protein homologous transcription factor (CHOP) (Zinszner et al., 1998) and activation of the apoptosis signal-regulating kinase 1/c-jun-N-terminal kinase pathway (Matsukawa et al., 2004) and cleavage of caspases 7, 9, and 12 (Haidara et al., 2008). The tribbles homolog 3 (TRB3) has been identified as a novel target of CHOP in ER stress response, and it seems to be involved in CHOP-dependent cell death as a second messenger (Ohoka et al., 2005).

The nuclear transcription factor-κB (NF-κB) is the major stress-inducible antiapoptotic transcription factor (Bowie and O'Neill 2000). NF-κB activation is associated with cancer, and it has been found to be strongly activated in many types of cancer, including HCC (Liu et al., 2002). Dehydroxymethylepoxyquinomicin (DHMEQ) is a novel NF-κB inhibitor (Umezawa and Chaicharoenpong 2002) that induces apoptosis and cell-cycle arrest in several cancer cell types (Starenki et al., 2004; Nishimura et al., 2006; Poma et al., 2006). DHMEQ also inhibits functional differentiation of bone marrow-derived macrophages into macrophages (Suzuki et al., 2008). However, the molecular mechanism(s) responsible for DHMEQ activity in cancer cells are not well understood. Therefore, the present study was set up to elucidate the molecular mechanisms by which DHMEQ exerts its anticancer effects against human liver cancer cells. We demonstrate that DHMEQ promotes ROS generation that in turn inhibited cell growth and proliferation, and increased apoptosis. Moreover, we found that DHMEQ causes activation of ER stress response, leading to cell growth inhibition. DHMEQ-induced ROS production also provoked DNA damage in liver cancer cells. The inhibition of all these effects by the antioxidant *N*-acetyl-L-cysteine (NAC) strongly provides evidence that antitumor effects by DHMEQ are mediated mainly through oxidative stress.

Materials and Methods

Cell Lines and Cell Culture. The well differentiated human hepatoblastoma cell line HuH-6 and the poorly differentiated human hepatocellular carcinoma cell line HA22T/VGH used in this study were of a low passage number and were maintained in RPMI 1640 medium supplemented with penicillin/streptomycin, sodium pyruvate, and L-glutamine, and containing 10% (v/v) fetal bovine serum (FBS). The two cell lines have different characteristics of differentiation, biological behavior, and genetic defects (Cervello et al., 2004a).

Chemicals. DHMEQ was synthesized as described previously (Suzuki et al., 2004). Dantrolene, EGTA, BAPTA-AM, rotenone, apocynin, antimycin, oligomycin, thenoyltrifluoroacetone (TTFA), sodium azide, trolox, allopurinol, quinacrine, and diphenyleneiodonium (DPI) were purchased from Sigma Aldrich (Milan, Italy) and U0126 from Alexis Biochemicals (Florence, Italy).

Cell Growth Assay. Cells (5×10^3/well) were distributed into each well of 96-well microtiter plates and then incubated overnight. At time 0, the medium was replaced with fresh complete medium, containing 10% FBS and in some cases different doses of DHMEQ, and the cells were cultured for 24, 48, and 72 h. For combined treatment, cells were pretreated with antioxidants or different inhibitors and then in their presence treated with DHMEQ. In particular, cells were pretreated with NAC for 2 h or with BAPTA-AM, EGTA, dantrolene, rotenone, TTFA, antimycin, sodium azide, oligomycin, apocynin, DPI, quinacrine, allopurinol, U0126, and 6-hydroxy-2,5,7,8-tetramethylchroman-2-carboxylic acid for 1 h. At the end of treatment, MTS assays were performed using the CellTiter Aqueous OneSolution kit (Promega Corporation, Madison, WI) according to the manufacturer's instructions. Cytotoxicity was expressed as a percentage of the absorbance measured in the control cells. Values were expressed as means ± S.D. of three separate experiments, each performed in triplicate.

BrdU Incorporation Assay. Cell proliferation was determined by estimating the amount of bromodeoxyuridine (BrdU) incorporation into DNA by a colorimetric immunoassay (Roche Diagnostics GmbH, Mannheim, Germany). In brief, 2.5×10^3 cells were cultured in 96-well plates in the different concentrations of DHMEQ for 24 h. BrdU (final concentration, 10 μM) was then added. The cells were then reincubated for an additional 24 h and subsequently fixed and incubated with anti-BrdU peroxidase according to the manufacturer's instructions. Color was developed by the addition of tetramethylbenzidine substrate and measured at 490 nm. Color intensity and absorbance values directly correlated to the amount of BrdU incor-

porated into DNA. Results were expressed as percentage inhibition of BrdU incorporation over the control. Values were expressed as means ± S.D. of three separate experiments, each performed in triplicate.

NF-κB p65 Transcription Factor Assay. Cytoplasm and nuclear extracts from 2×10^6 cells treated or untreated with DHMEQ were prepared using Nuclear Extract Kit (Active Motif, Rixensart, Belgium) according to the manufacturer's instructions. The DNA-binding capacity of NF-κB (p65 subunit) was measured using Trans-AM kit (Active Motif) according to the manufacturer's instructions. In brief, 25 μg of nuclear protein samples were distributed in a 96-well plate and incubated with primary antibody against NF-κB p65. A secondary HRP-conjugated antibody provides a sensitive colorimetric readout quantified by spectrophotometry. Results were expressed as percentage inhibition of binding over the control. Values were expressed as means ± S.D. of three separate experiments, each performed in duplicate.

Caspase Activity Assays. Cells (2×10^4/well) were pretreated with or without the scavenger NAC for 2 h and then treated with DHMEQ. After 6 h, the levels of caspase activities in the cells were measured by the Caspase-Glo 3/7, Caspase-Glo 8, and Caspase-Glo 9 assays (Promega, Milan, Italy) according to the manufacturer's instructions. Results were expressed as -fold induction over the control. Values were expressed as means ± S.D. of three separate experiments, each performed in duplicate.

Western Blot Analysis. Whole cellular lysates from 1.5×10^6 cells were obtained using radioimmunoprecipitation assay buffer (Cell Signaling Technologies Inc., Danvers, MA) and Western blotting were performed as described previously (Cervello et al., 2004b), with primary antibodies raised against survivin (Abcam Limited, Cambridge, UK), β-actin (Sigma-Aldrich Srl, Milan, Italy), phospho-ERK, and poly(ADP-ribose) polymerase (PARP; Cell Signaling Technologies Inc.),

Cytochrome *c* Release. Cells (2×10^6) were pretreated with or without the scavenger NAC for 2 h and then, in its presence, cells were treated or untreated with DHMEQ. Then, cells were collected and lysed in a hypotonic lysis buffer on ice for 20 min (200 mM HEPES, 1 mM EDTA, 1 mmol EGTA, 1.5 mM $MgCl_2$, 10 mM KCl, 1 mM dithiothreitol, 250 mM sucrose, 0.1 mM phenylmethylsulfonyl fluoride, 10 μg/ml aprotinin, leupeptin, and pepstatin A). The lysates were centrifuged at 10,000*g* for 20 min at 4°C. The supernatant (cytosol) was collected. The pellets were lysed with radioimmunoprecipitation assay buffer (Cell Signaling Technologies Inc.) on ice for 20 min and then further centrifuged at 10,000*g* for 20 min at 4°C. The supernatants that contained mitochondria were collected. Proteins concentration was determined using the micro-protein assay from Bio-Rad Laboratories (Milan, Italy). Aliquots of 25 μg of proteins were analyzed by Western blotting with primary antibodies raised against cytochrome *c* (BD Pharmingen, San Diego, CA) and anti-peroxiredoxin 3 (Sigma-Aldrich). β-Actin immunolabeling and Red-Ponceau staining were performed as loading controls for the cytoplasmic and the mitochondrial fractions, respectively.

RT-PCR. Total RNA was isolated from 2×10^5 cells using Trizol reagent (Invitrogen, Carlsbad, CA) as recommended by the supplier. Total RNA (1.5 μg) was subjected to reverse transcription to generate cDNA. To analyze human GRP78, TRB3, CHOP, XBP1, and β-actin mRNA expression levels, semiquantitative PCR was performed using specific 5′ and 3′ primers that generated specific bands (Table 1). Amplification of cDNA was performed with the number of cycles and annealing temperatures reported in the Table 1. The expression of β-actin served as an internal control. Aliquots of the PCR products were fractionated by electrophoresis through 1.6% agarose gels containing ethidium bromide, visualized, and quantified by densitometric scanning.

siRNA Transfection. HA22T/VGH cells (2×10^5) were transfected with TRB3 and noncorrelated siRNA SMARTPool ON-Target plus (Dharmacon Inc., Lafayette, CO) according to the manufacturer's instructions. In brief, cells were seeded onto 60-mm dishes in medium without antibiotics; 24 h later, the transfection of siRNAs was carried out with DharmaFECT 4 (Dharmacon Inc.). All transfections were carried out with 20 μM duplex siRNA in medium without FBS and antibiotics. After 24 h, cells were split into 96-well plates to perform MTS assays and in 60-mm dishes for TRB3 mRNA analysis.

Flow Cytometry Analysis. After 24 h of DHMEQ treatment, 10^6 cells were collected and stained with propidium iodide (Invitrogen), and the percentage of apoptotic cells was determined as described previously (Cervello et al., 2004b).

Measurement of Reactive Oxygen Species. The intracellular accumulation of ROS was determined using the fluorescent probe 2′,7′-difluorodihydrofluorescein diacetate (H_2DCFDA) (Invitrogen). Cells (3×10^5) were treated with various concentrations of DHMEQ in the presence or absence of NAC (2 mM) for 16 h. Cells were collected, resuspended in PBS with calcium, and incubated with the probe (1μM) in the dark at 37°C, 5% CO_2 for 15 min. The fluorescence was measured by flow cytometry. Data are expressed as the percentage of positive cells.

Immunofluorescence of γ-H2AX. HA22T/VGH and HuH-6 cells were distributed into eight-well chamber slides and treated or untreated with DHMEQ in the presence or absence of 2 mM NAC for 16 h. Cells were fixed with in a 1:1 (v/v) acetone/methanol solution mixture and rehydrated in PBS. Cells were incubated with rabbit anti-human-γ-H2AX (1:500; Enzo Biosciences, Farmingdale, NY) and then incubated with anti-rabbit Alexa Fluor 488-conjugated secondary antibody (1:1000; Invitrogen), rinsed twice with PBS, counterstained with 4,6-diamidino-2-phenylindole, and mounted. Immunofluorescence was visualized using a Zeiss Axiophot microscope.

Statistical Analysis. Statistical analysis was performed using Student's two-tailed *t* test. The criterion for statistical significance was $p < 0.05$.

Results

DHMEQ Reduces NF-κB p65 DNA-Binding Capacity, Cell Growth, and Induces Apoptosis in Human Hepatoma Cells. DHMEQ has been reported to inhibit NF-κB p65 translocation into the nucleus in many cell types (Ariga et al., 2002), affects cellular proliferation and differentiation (Starenki et al., 2004; Nishimura et al., 2006; Poma et al., 2006; Suzuki et al., 2008), and displayed anti-tumor effects in vivo (Umezawa 2006). However, the

TABLE 1
Sequences of oligonucleotide primers and PCR conditions

Gene Name	Forward Oligonucleotide	Reverse Oligonucleotide	Size	AT	Cycle Numbers
			bp	*°C*	
GRP78	gacatcaagttcttgccgtt	ctcataacatttaggccagc	259	58	40
CHOP	atggcagctgagtcattgcc	tcatgcttggtgcagattc	509	58	30
TRB3	gccactgcctcccgtcttg	gctgccttgcccgagtatga	538	58	30
XBP1	ccttgtagttgagaaccagg	ggggcttggtatatatgtgg	423	57	32
β-actin	caccacaccttctacaatgagc	gaggatcttcatgaggtagtcagtc	321	60	22

bp, base pairs; AT, annealing temperature.

molecular mechanism(s) of DHMEQ-induced antitumor effects in cancer cells are not well understood. Therefore, in the present study, we investigated the effects of DHMEQ in two human hepatoma cell lines, HA22T/VGH and HuH-6. We first determined whether DHMEQ inhibited NF-κB transcriptional activity in hepatoma cells. As shown in Fig. 1A, DHMEQ dose-dependently decreased the amount of the active form of p65 subunit contained in nuclear extracts in both cell lines.

The MTS assays were used to assess the effects of DHMEQ on cell growth. HA22T/VGH and HuH-6 cells were exposed to increasing concentrations of DHEMQ for different times. After 48 h, the dose-response study showed that HuH-6 cells were more responsive to DHMEQ than HA22T/VGH cells (Fig. 1B). After 72 h of exposure to the drug, the IC_{50} values were 12.5 and 32.5 μg/ml in HuH-6 and HA22T/VGH, respectively.

BrdU assays were performed to study the effects of DHMEQ on cell proliferation. The results in Fig. 1C demonstrated that DHMEQ affects cell proliferation in a dose-dependent manner in both cell lines. Again, HuH-6 cells were more responsive to the inhibitory effects of DHMEQ.

To investigate whether DHMEQ induced apoptosis in human hepatoma cells, we analyzed by Western blotting the induction of cleavage of PARP, a known caspase-3 substrate and a biochemical marker of apoptosis, and the level of the antiapoptotic protein survivin. Figure 1D shows that DHMEQ treatment induced PARP cleavage in both cell lines, suggesting activation of caspase cascades, and it reduced the level of survivin. Apoptosis was also evaluated by flow cytometry analysis of DNA stained with propidium iodide and by determining the percentage of events accumulated in the pre-G_o-G_1 position (Fig. 1E). A significant increase in the percentage of apoptosis was observed in DHMEQ treated HuH-6 cells.

DHMEQ Enhances the Phosphorylation of ERK1/2 and, in Combination with the MEK-Specific Inhibitor U0126, Reduces Cell Growth. Because ERK1/2 are involved in cell proliferation and apoptosis, we examined by Western blotting analysis the levels of phosphorylated (activated) forms of ERK1/2 in cells treated with different concentrations of DHMEQ. As shown in Fig. 2A, DHMEQ induced ERK1/2 phosphorylation in both cell lines in a dose-dependent manner. To evaluate the role of mitogen-activated protein kinase activation after DHMEQ treatment, we used a

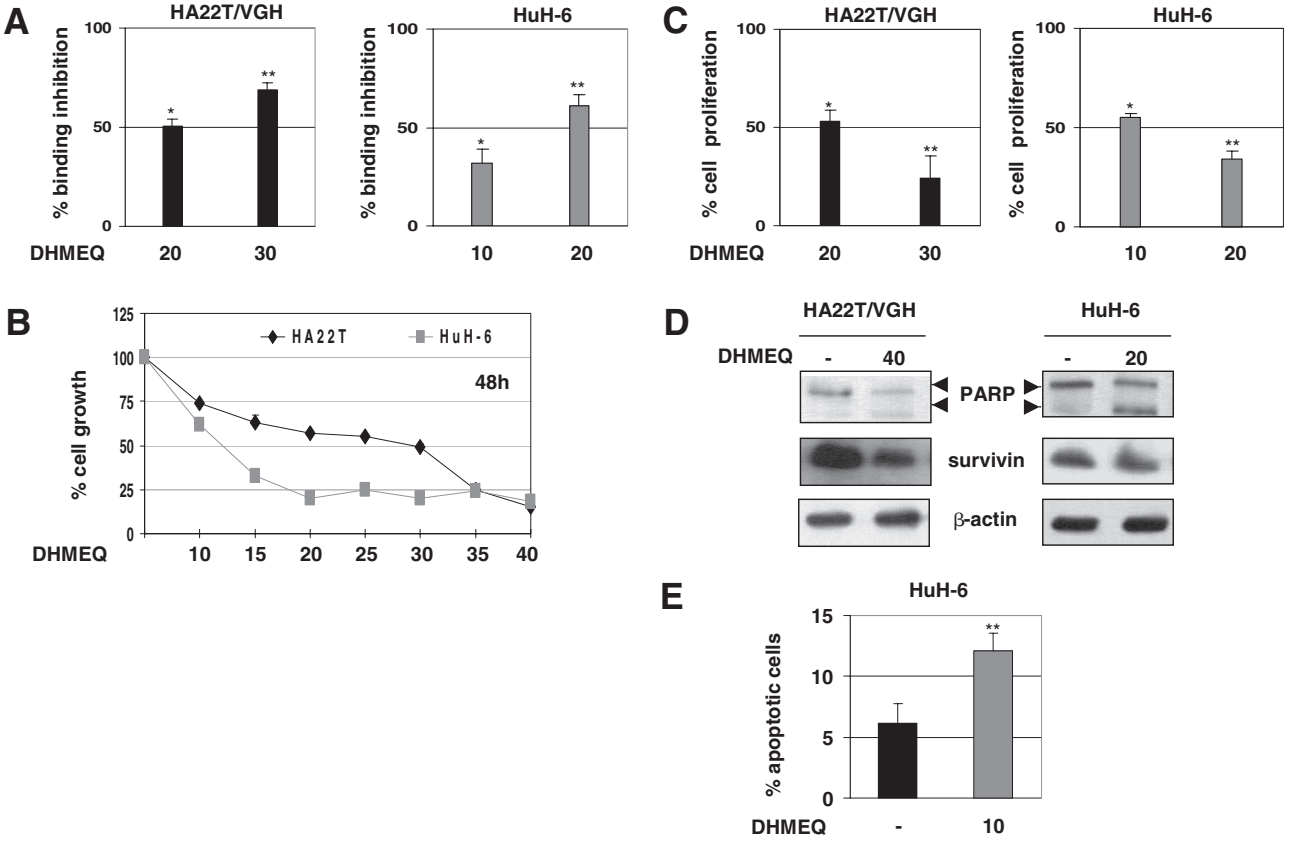

Fig. 1. DHMEQ inhibits NF-κB p65 DNA-binding capacity and cell growth and induces apoptosis in human hepatoma cells. A, HA22T/VGH and HuH-6 cells were treated with the indicated concentrations of DHMEQ (micrograms per milliliter) for 16 h. The NF-κB active form (p65 subunit) contained in the nuclear fraction was measured by TRANS-AM assays. Data are expressed as percentages of p65 binding inhibition of the control cells and are the means ± S.D. of three separate experiments. *, $p < 0.05$; **, $p < 0.01$ versus control. B, cell growth was assessed by MTS assays. Cells were treated with different concentrations of DHMEQ (micrograms per milliliter) for the indicated times. Data are expressed as the percentage of control cells and are the means ± S.D. of three separate experiments, each of which was performed in triplicate. C, cell proliferation was assessed by BrdU assay. Cells were treated with DHMEQ (micrograms per milliliter) for 24 h. Data are expressed as the percentage of the control cells and are the means ± S.D. of three separate experiments. *, $p < 0.05$; **, $p < 0.01$ versus control. D, HuH-6 and HA22T/VGH cells were treated or untreated for 24 h with 20 and 40 μg/ml DHMEQ, respectively. After treatment, cells were harvested and lysed, and equal amounts of extracted proteins were analyzed for induction of PARP cleavage and survivin expression by immunoblotting. The data shown represent three independent experiments with comparable outcomes. Arrowheads indicate the 115- and 85-kDa forms of PARP. E, HuH-6 cells were treated or untreated with 10 μg/ml DHMEQ for 24 h, and cell death was determined by flow cytometry analysis of subgenomic DNA. Data are expressed as percentages of apoptotic cells and are the mean ± S.D. of three separate experiments. **, $p < 0.01$ versus control.

MEK inhibitor, U0126, and analyzed its effect on cell growth by a MTS assay. Cells were pretreated with U0126 (2 μM) for 1 h and then, in its presence, cells were treated with different concentrations of DHMEQ for 24 h. Combination of U0126 with DHMEQ significantly reduced cell growth in both cell lines (Fig. 2B), suggesting that the MEK/ERK pathway is activated as a pro-survival signaling during DHMEQ treatment.

DHMEQ Triggers ER Stress Response in a Ca^{2+}-Independent Manner. Accumulating evidence suggests that the ER also is an important apoptotic control point (Danial and Korsmeyer, 2004). CHOP, the spliced form of XBP1(sXBP1), and TRB3 are transcription factors whose expression is induced during ER stress response and participate in ER-mediated apoptosis. To examine whether DHMEQ activated ER stress response in human hepatoma cells, we determined the effects of DHMEQ on the expression of ER stress genes *GRP78*, *CHOP*, *XBP1*, and *TRB3*. Cells were treated for 6 h with different concentrations of DHMEQ and then the levels of these mRNAs were examined by RT-PCR analysis. Experiments revealed that substantial induction of CHOP and TRB3 mRNA were detected already at 6 h in both cell lines; in contrast, GRP78 was enhanced only in HA22T/VGH cell (Fig. 3A). Furthermore, DHMEQ-treatment induced XBP1 mRNA splicing in a dose-dependent manner in both cell lines. These results suggest that ER stress is activated in response to DHMEQ treatment.

Increases in the intracellular Ca^{2+} concentration promote apoptosis through ER stress response (Choi et al., 2007) and through induction of CHOP expression (Oydomari and Mori 2004). Therefore, to examine the role of Ca^{2+} on cell growth in DHMEQ-treated cells, we used BAPTA-AM and EGTA as intracellular Ca^{2+}chelators and dantrolene as inhibitor of Ca^{2+} release from sarcoplasmic reticulum. Figure 3B shows that BAPTA-AM and EGTA alone partially affect cell growth in HA22T/VGH cells, and dantrolene partially affects cell growth only in HuH-6 cells. In HA22T/VGH, preincubation with Ca^{2+} chelators followed by DHMEQ treatment had negligible effects on cell growth, suggesting that DHMEQ induced apoptosis in a Ca^{2+}-independent manner. This was further supported by the observation that preincubation with dantrolene did not modify the growth inhibitory effects of DHMEQ in both cell lines (Fig. 3B).

TRB3 siRNA Transfection Reverts DHMEQ-Induced Cell Growth Inhibition. TRB3, a crucial factor that mediates the ER stress response, is a transcriptional target of CHOP and seemed to be involved in CHOP-dependent cell death as a second messenger during ER stress (Ohoka et al., 2005). To examine the role of TRB3 in DHMEQ-induced cell growth inhibition, HA22T/VGH cells were first transiently transfected with siRNA specific for TRB3 for 72 h and then MTS assays were performed after 24 h of treatment with DHMEQ. The transfection of TRB3 siRNA into HA22T/VGH cells effectively reduced the endogenous mRNA by more than 75% compared with control siRNA (Fig. 4A). As shown in Fig. 4B, knockdown of TRB3 in HA22T/VGH cells significantly reverted the inhibition of cell growth induced by DHMEQ treatment. These results suggest that activation of ER stress response, through TRB3 mRNA up-regulation, has an important role in the DHMEQ-induced cell growth inhibition.

DHMEQ Induces Apoptosis through ROS Species Generation. A number of studies show that induction of oxidative stress and ROS generation in cells are effective apoptotic inducers (von Harsdorf et al., 1999; Buccellato et al., 2004). Accordingly, we investigated whether DHMEQ antitumor activities in hepatoma cells are initiated through ROS generation. Cells were treated with different concentrations of DHMEQ for 16 h; thereafter, ROS generation was measured

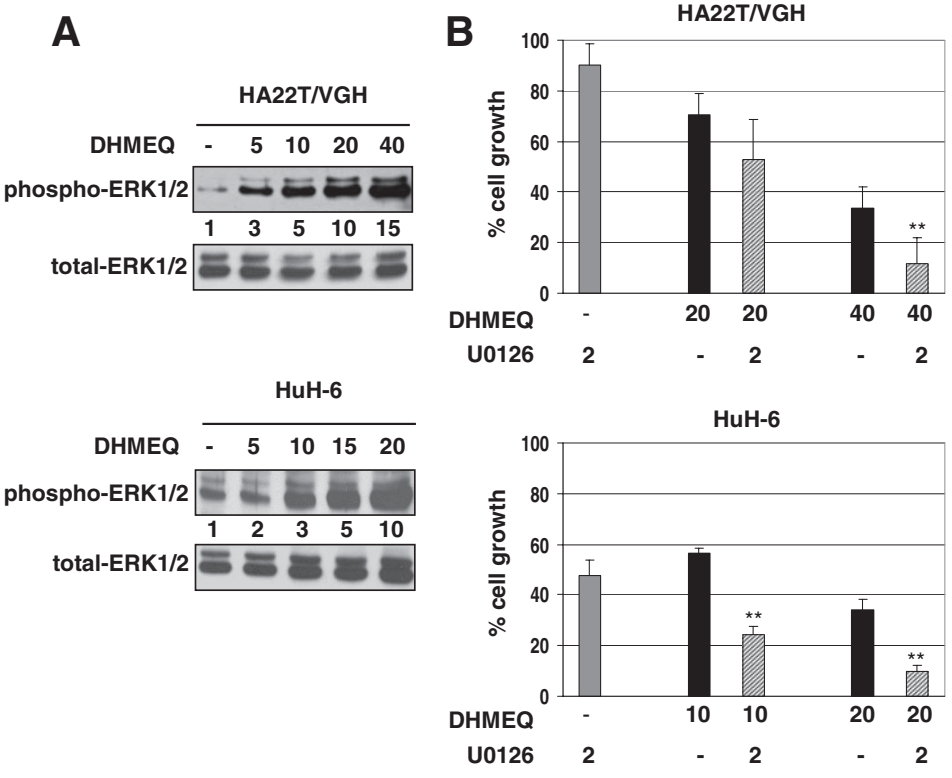

Fig. 2. DHMEQ activates ERK1/2 in hepatoma cells and its combination with U0126 decreases cell growth. A, HA22T/VGH and HuH-6 cells were treated with DHMEQ (micrograms per milliliter) for 24 h at the indicated concentrations. After treatment, cells were harvested and lysed, and equal amounts of proteins were analyzed for total and phospho-ERK1/2 expression by immunoblotting analysis. The numbers represent -fold of phospho-ERK1/2 difference with vehicle-treated control samples (−) arbitrarily set at 1.0. The data shown represent three independent experiments with comparable outcomes. B, cell growth was assessed by MTS assays. HA22T/VGH and HuH-6 cells were treated with DHMEQ (micrograms per milliliter) for 24 h. In the combination experiments, the cells were exposed to the specific MEK inhibitor U0126 (2 μM) for 1 h and then coexposed to DHMEQ for a further 24 h. Data are expressed as the percentage of control cells and are the means ± S.D. of three separate experiments, each of which was performed in triplicate. **, $P < 0.01$ versus each agent alone.

using the cell-permeable fluorescent probe H_2DCFDA. As shown in Fig. 5A, treatment of HA22T/VGH cells with DHMEQ in a dose-dependent manner promotes ROS generation. In the same experiment we have examined the effect of the antioxidant NAC on DHMEQ-induced ROS generation. For this purpose, cells were pretreated with 2 mM NAC for 2 h and then, in its presence, cells were treated with DHMEQ for 16 h. As shown in Fig. 5A, pretreatment with NAC drastically decreased DHMEQ-induced ROS production in HA22T/VGH cells. To confirm that DHMEQ induces cell death through an oxidant action, we used the synthetic of vitamin E analog 6-hydroxy-2,5,7,8-tetramethylchroman-2-carboxylic acid, which is known for its antioxidant properties (Chen et al., 2008). Figure 5B showed that pretreatment with 50 μM 6-hydroxy-2,5,7,8-tetramethylchroman-2-carboxylic acid for 1 h significantly reverted cell growth inhibition induced by DHMEQ.

The major sources of ROS are the mitochondrial respiratory chain (MRC) components (Richter and Schweizer 1997), the enzymes xanthine/xanthine oxidase (McCord, 1985), the NADPH oxidase (Trudel et al., 1991), and the phospholipase A_2-activated arachidonic acid metabolism (Henderson et al., 1989). To determine the source(s) of ROS in cells treated with

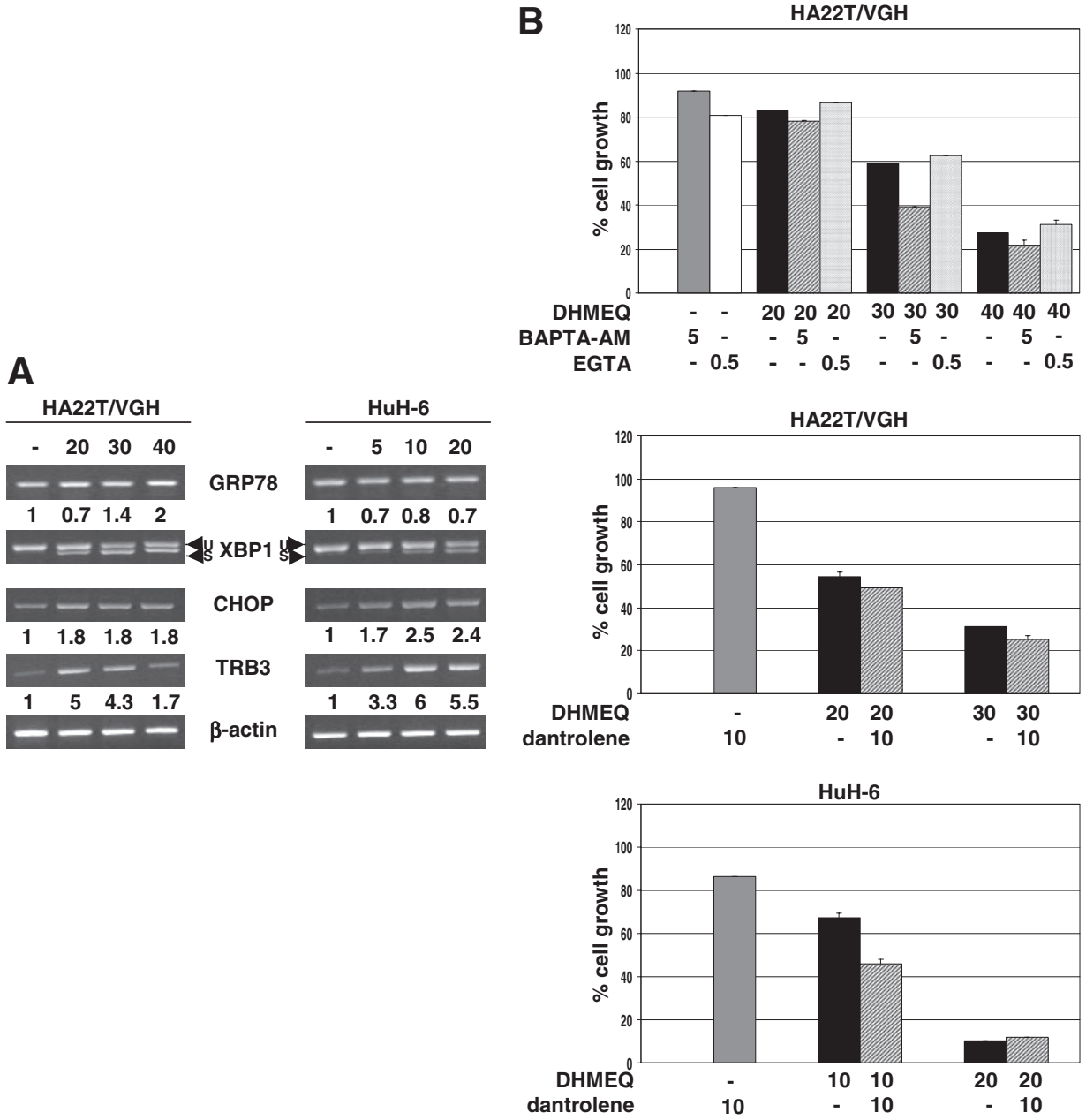

Fig. 3. DHMEQ triggers ER stress response in a Ca^{2+}-independent manner. A, cells were treated with different concentrations of DHMEQ (micrograms per milliliter) for 6 h, and then mRNA expression levels of genes involved in the ER stress response were analyzed by RT-PCR analysis. For XBP1 mRNA, the unspliced (U) and the spliced (S) forms are indicated by arrowheads. The numbers represent the ratio of the relevant mRNA normalized with β-actin, with vehicle-treated control samples (−) arbitrarily set at 1.0. The data shown represent three independent experiments with comparable outcomes. B, cell growth was assessed by the MTS assay. HA22T/VGH and HuH-6 cells were incubated in the presence of the indicated concentrations of DHMEQ (μg/ml). In the combination experiments, the cells were exposed to BAPTA-AM, EGTA, and dantrolene for 1 h and then coexposed to DHMEQ for an additional 24 h. Data are expressed as the percentage of control cells and are the means ± S.D. of three separate experiments, each of which was performed in triplicate.

DHMEQ, we analyzed the effects of various ROS generation inhibitors. We used DPI and apocynin as the inhibitors of NADPH oxidase, allopurinol as an inhibitor of xanthine/xanthine oxidase and quinacrine as an inhibitor of phospholipase A_2. Cells were pretreated for 1 h with a single inhibitor and then in its presence treated with DHMEQ (30 μM) for 6 h. All of them failed to revert cell growth inhibition induced by DHMEQ. (data not shown). Next, we analyzed the effects of several inhibitors of MRC complexes I to V using concentrations that are not toxic to the cells, because it has been reported that these inhibitors may also increase ROS production in many cell types and cause cell death (Riganti et al., 2006; Chen et al., 2007) (data not shown). The MRC complex I inhibitor rotenone (1 μM) and complex II inhibitor TTFA (0.1 mM) failed to inhibit DHMEQ-induced cell growth reduction. On the contrary, the combination of these inhibitors with DHMEQ significantly increased cell growth inhibition in both cell lines (data not shown). The results in Fig. 5B showed that complex III inhibitor antimycin (1 μg/ml), complex IV inhibitor sodium azide (0.5 mM), and complex V inhibitor oligomycin (0.5 μg/ml) significantly reverted DHMEQ-induced reduction of cell growth, demonstrating that mitochondria are the major cellular source of ROS.

ROS generation can also lead to disruption of the mito-

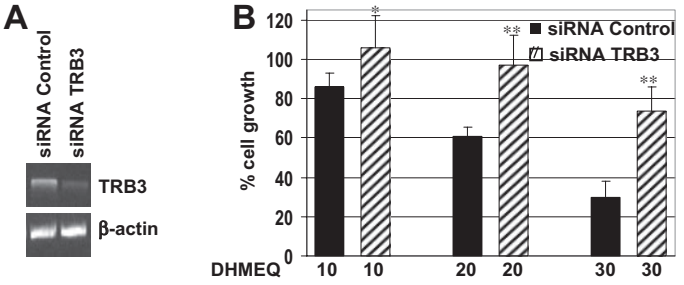

Fig. 4. TRB3 siRNA transfection reverts DHMEQ-induced cell growth inhibition. HA22T/VGH cells were transfected with a control siRNA (siRNA C) or TRB3-selective siRNA (siRNA TRB3). Seventy-two hours after transfection, cells were treated or untreated for 24 h with DHMEQ (micrograms per milliliter) at different concentrations, and the cell growth was determined by MTS assays. Results are expressed as the percentage of cell growth relative to the vehicle-treated cells and are the means ± S.D. of three separate experiments each of which was performed in triplicate. *, $p < 0.05$; **, $p < 0.01$ versus control siRNA.

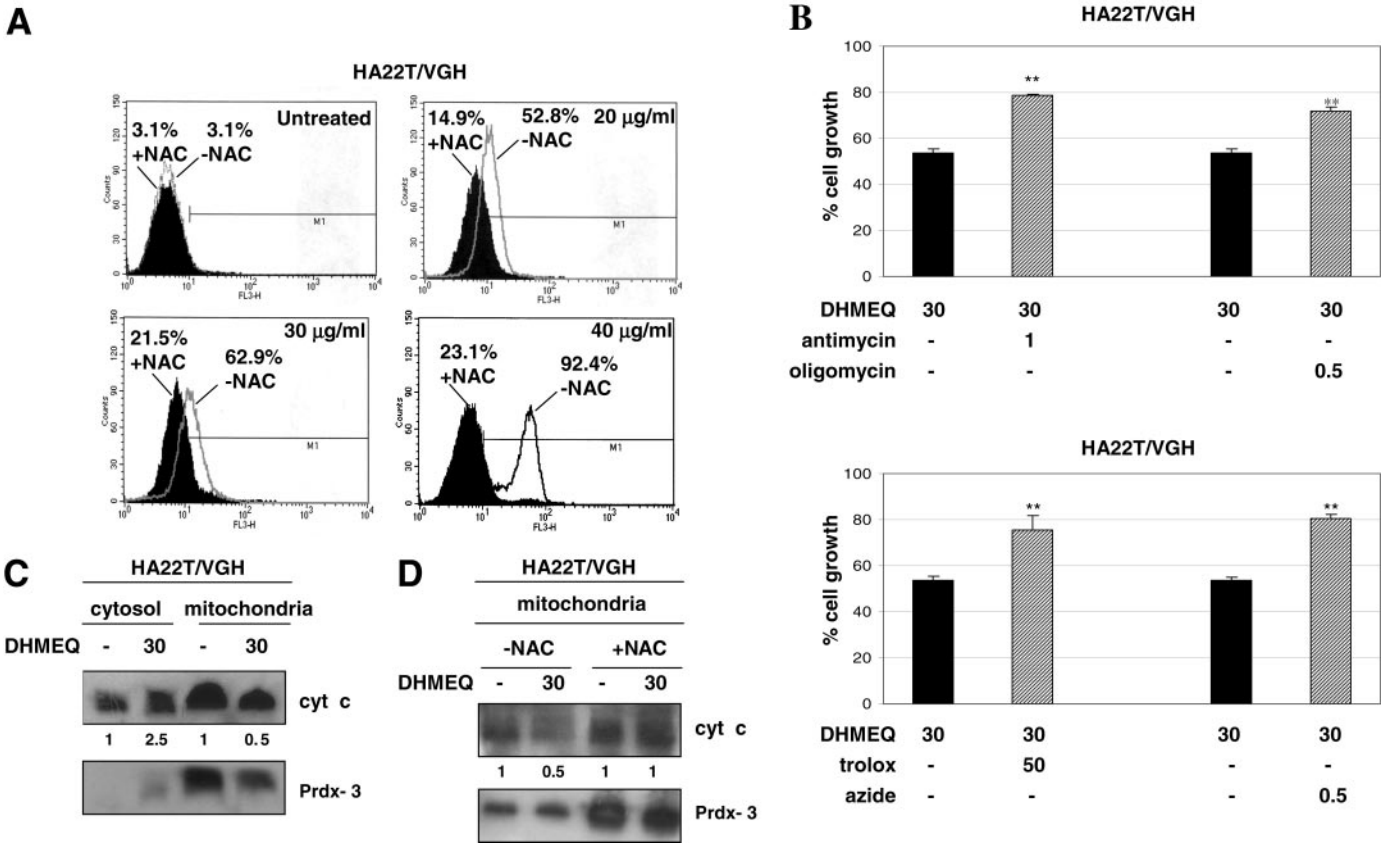

Fig. 5. DHMEQ induces ROS generation and ROS-dependent release of cytochrome *c*. A, HA22T/VGH cells were treated or untreated with indicated concentrations of DHMEQ for 16 h with or without the presence of the antioxidant NAC (2 mM). The cells were harvested and incubated with the fluorescent probe H_2DCFDA, and the fluorescence was measured by flow cytometry. Data are expressed as percentages of positive cells measured in each experimental conditions and are representative of two different experiments. B, cell growth was assessed by MTS assay. Cells were pretreated with antimycin (micrograms per milliliter), oligomycin (micrograms per milliliter), sodium azide (micromolar) and antioxidant 6-hydroxy-2,5,7,8-tetramethylchroman-2-carboxylic Acid (Trolox; micromolar) for 1 h and then, in their presence, cells were treated with DHEMQ (micrograms per milliliter) for 6 h. Data are expressed as the percentage of control cells and are the means ± S.D. of three separate experiments, each of which was performed in triplicate. **, $p < 0.01$ versus each agent alone. C, cells were treated with 30 μg/ml DHMEQ for 24 h and then cytoplasmic and mitochondrial fractions were separated and analyzed by Western blotting for cytochrome *c* and Prdx-3 expression. β-Actin immunolabeling and Red-Ponceau staining were performed as loading controls for the cytoplasmic and the mitochondrial fractions, respectively (not shown). The numbers represent -fold protein difference with vehicle-treated control samples (−) arbitrarily set at 1.0. The data shown represent two independent experiments with comparable outcomes. D, cells were pretreated for 2 h with or without 2 mM NAC and then with 30 μg/ml DHMEQ for 24 h. The mitochondrial fraction was analyzed by Western blotting for cytochrome *c* and Prdx-3 expression. The numbers represent -fold cytochrome *c* difference with vehicle-treated control samples (−) arbitrarily set at 1.0. The data shown represent two independent experiments with comparable outcomes.

chondrial membrane potential and consequently might provoke release of cytochrome *c* into the cytosol. To examine whether cytochrome *c* release also occurred in DHMEQ-treated hepatoma cells, Western blotting analysis was performed. As expected, after 24 h of treatment with DHMEQ, an increase in the amount of cytochrome *c* was detected in the cytosolic fraction in both cell lines (Fig. 5C). Accordingly, a decrease in the amount of cytochrome *c* was observed in the mitochondrial fraction (Fig. 5C). Pretreatment with antioxidant NAC prevented the cytochrome *c* release from the mitochondria (Fig. 5D). These results imply that DHMEQ induces ROS, which leads to mitochondrial dysfunction and subsequently the release of an apoptogenetic factor.

We then examined the expression of the antioxidant protein Peroxiredoxin-3 (Prdx-3), a mitochondrial member of the antioxidant family of thioredoxin peroxidases. Prdx-3 protects cells against ROS-induced damage and regulates cytochrome *c* release (Nonn et al., 2003). As shown in Fig. 5C, Prdx-3 increased in the DHMEQ-treated cytosolic fraction and decreased in the mitochondrial fraction.

DHMEQ Induces DNA Damage through ROS Production. ROS are well known to induce damage of a variety of biomolecules, such as DNA, RNA, and protein. To evaluate whether DHMEQ treatment could lead to DNA damage, we examined the phosphorylation of H2AX (γ-H2AX), which has been recently considered an index of the production of double-strand breaks. Therefore, HA22T/VGH and HuH-6 cells were treated with DHMEQ with or without NAC for 2 h. After 16 h of DHMEQ treatment, the presence of DNA damage was analyzed by immunofluorescence. As shown in Fig. 6 DHMEQ induced accumulation of the phosphorylated form of histone H2AX (γ-H2AX) in nuclear foci in both cell lines, and NAC prevented the DNA damage. These results indicate that DHMEQ induces oxidative DNA damage through the production of ROS.

The Antioxidant NAC Abrogates DHMEQ-Induced Apoptosis, Cell Growth Inhibition, Phosphorylation of ERK1/2, and ER Stress Response. To determine whether DHMEQ induced apoptosis via ROS generation, we tested the effects of NAC on caspase activation in both cell lines. Cells were pretreated with 2 mM NAC for 2 h and subsequently in the presence of NAC treated with different concentrations of DHMEQ for an additional 6 h. We measured caspase activation with ELISA assays. As shown in Fig. 7A, treatment with DHMEQ induced activation of caspases-3/7, -8, and -9 in both cell lines, and NAC markedly suppressed their activation. Moreover, we analyzed by Western blotting the cleavage of PARP and the level of the antiapoptotic protein survivin. Cells were pretreated with NAC for 2 h and then, in its presence, treated with different concentrations of DHMEQ for 24 h. DHMEQ promoted proteolytic cleavage of PARP and decreased the level of survivin in a dose-dependent fashion (Fig. 7B). Treatment with NAC abrogated the cleavage of PARP and restored the expression of survivin in

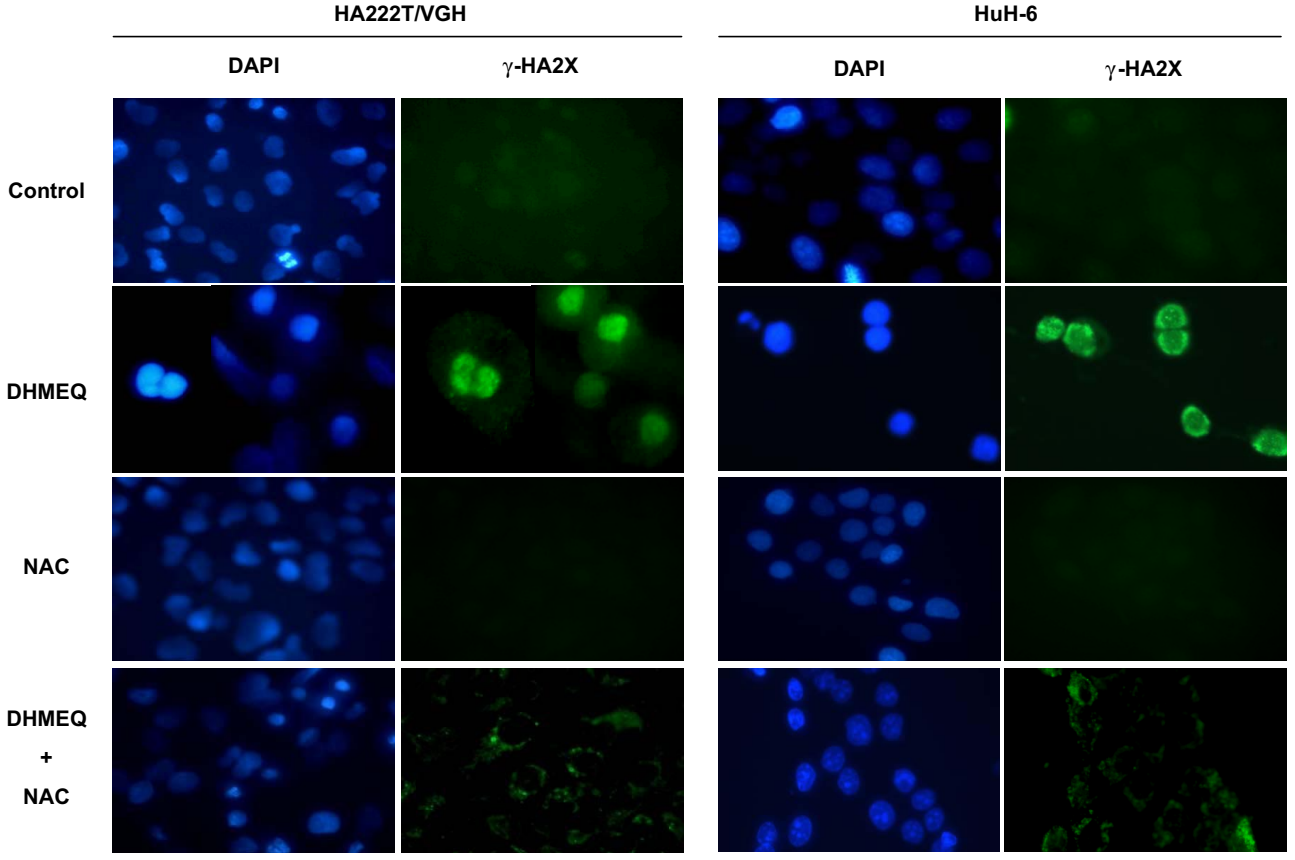

Fig. 6. DHMEQ induces DNA damage through ROS production. Cells were pretreated or not with the antioxidant NAC (2 mM) for 2 h, and then HA22T/VGH cells were treated with 30 μg/ml DMHEQ and HuH-6 cells with 20 μg/ml DHMEQ for 16 h. DNA damage was detected by accumulation in the nuclear foci of the phosphorylated form of histone H2AX (γ-H2AX). The data shown represent two independent experiments with comparable outcomes.

both cell lines. These results indicate that DHMEQ triggers apoptosis through ROS production.

Next, we examined the effects of ROS generation on cell growth by MTS assays in the presence of NAC. Treatment of HA22T/VGH and HuH-6 cells with DHMEQ for 24 h reduced cell growth in a dose-dependent manner; however, DHMEQ-reduced cell growth was prevented by pretreatment with NAC (Fig. 7C). These results indicate that DHMEQ inhibited hepatoma cell growth through production of ROS.

To address the relationship between MEK/ERK pathway and oxidative stress we analyzed the level of ERK1/2 phosphorylation induced by DHMEQ in the presence of NAC. Pretreatment with NAC blocked ERK1/2 phosphorylation induced by DHMEQ in both cell lines (Fig. 7D). These results indicate that activation of the pro-survival signaling MEK/ERK pathway was induced by ROS production.

Finally, to examine the relationship between ER stress response and oxidative stress after DHMEQ treatment, the induction of GRP78, CHOP, and TRB3 mRNAs and splicing of XBP1 mRNA was examined in the presence of NAC. Treatment with NAC abrogated induction of CHOP and TRB3 mRNAs in both cell lines, although GRP78 induction was abrogated only in HA22T/VGH cells (Fig. 7E). XBP1 mRNA splicing was inhibited by NAC treatment in both cell lines. These results indicate that the ER stress response is an event downstream of the oxidative stress induced by DHMEQ.

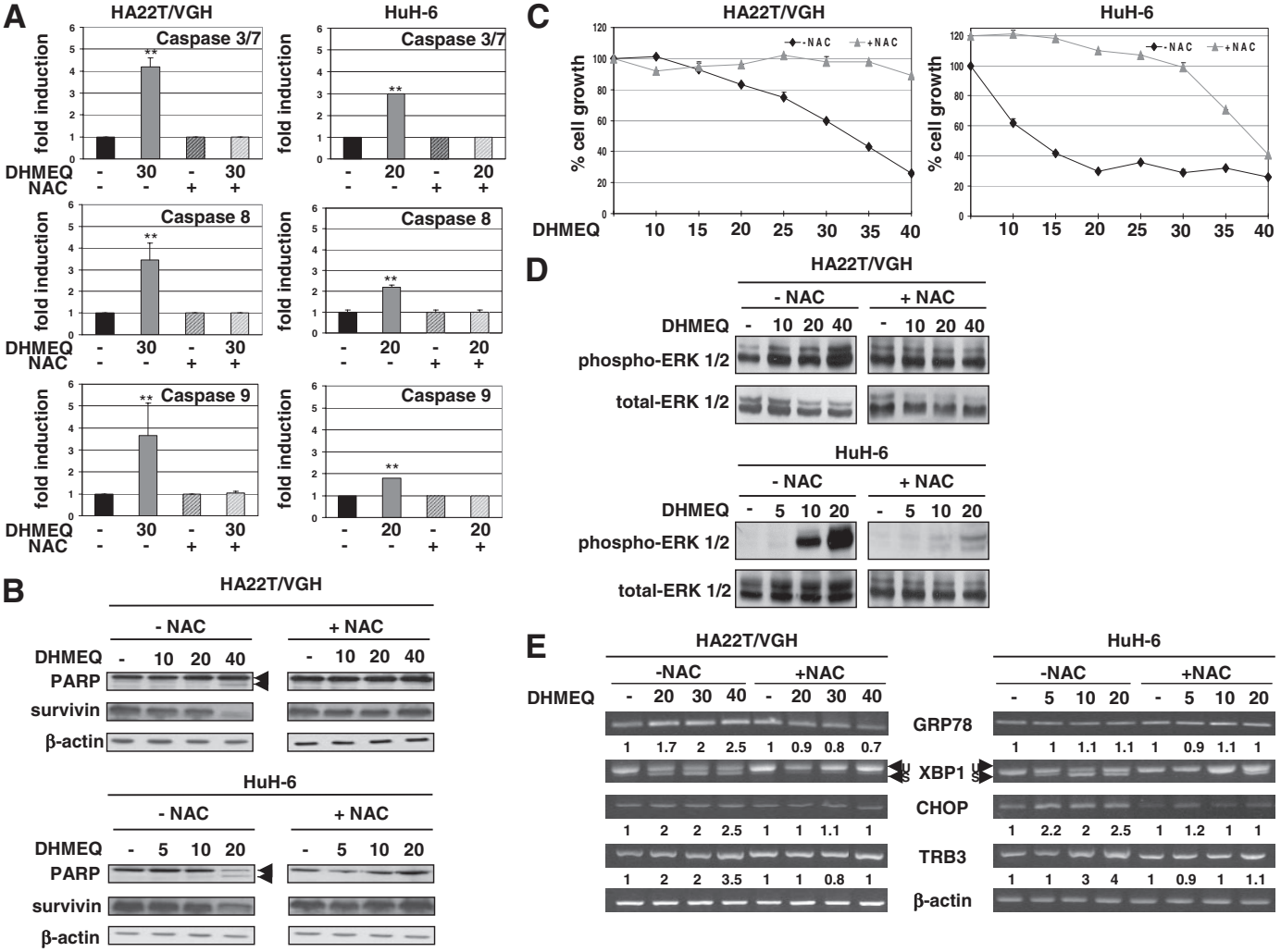

Fig. 7. The antioxidant NAC reverts DHMEQ-induced apoptosis, cell growth inhibition, ERK1/2 phosphorylation, and ER stress response. A, cells were pretreated with NAC (2 mM) for 2 h and then treated with different concentrations of DHMEQ (micrograms per milliliter) for 6 h. The levels of caspase activities in the cells were measured by the Caspase-Glo 3/7, Caspase-Glo 8, and Caspase-Glo 9 assays. Data are expressed as -fold increase of untreated cells and are the means ± S.D. of three separate experiments, each of which was performed in duplicate. **, $p < 0.01$ versus control. B, the induction of PARP cleavage and the levels of survivin proteins were analyzed by Western blotting. Cells were treated with different concentrations of DHMEQ (micrograms per milliliter) for 24 h with or without pretreatment with NAC (2 mM) for 2 h. The data shown represent three independent experiments with comparable outcomes. Arrowheads indicate the 115- and 85-kDa form of PARP. C, cell growth was assessed by MTS assays. HA22T/VGH and HuH-6 cells were pretreated with antioxidant NAC for 2 h and then treated with DHMEQ at the indicated concentrations (micrograms per milliliter) for 24 h. Data are expressed as the percentage of control cells and are the means ± S.D. of three separate experiments, each of which was performed in triplicate. D, phosphorylated levels of ERK1/2 were determined by Western blotting. Cells were treated with different concentrations of DHMEQ (micrograms per milliliter) for 24 h with or without pretreatment with NAC (2 mM) for 2 h. The data shown represent two independent experiments with comparable outcomes. E, HA22T/VGH and HuH-6 cells were treated with the indicated concentrations of DHMEQ (micrograms per milliliter) for 24 h with or without pretreatment of the antioxidant NAC (2 mM) for 2 h. mRNA expression was analyzed by RT-PCR. For XBP1 mRNA, the unspliced (U) and the spliced (S) forms are indicated by arrowheads. The numbers represent the ratio of the relevant mRNA normalized with β-actin, with vehicle-treated control samples (−) arbitrarily set at 1.0. The data shown represent two independent experiments with comparable outcomes.

Discussion

It has become increasingly evident that certain anticancer agents induce intracellular oxidative stress that is either the primary mechanism of cell death or is a secondary indirect effect that may lead to cell death. Cancer cells produce higher levels of ROS than do normal cells (Szatrowski et al., 1991). It is noteworthy that transformed cells are thought to use ROS signals to stimulate both cell proliferation and tumor progression. However, high levels of ROS, beyond a threshold, render cancer cells more vulnerable to apoptosis. Thus, agents that either promote ROS generation or decrease the levels of antioxidants have the potential to kill cancer cells with little effect on normal cells (Fang et al., 2007). Both the intensity and the duration of the oxidative stress stimulus determine the final response of the cells to the drug by regulating the kinetics and the diversity of the signaling or apoptotic pathways activated.

Oxidative stress may activate an ER stress response through up-regulation of ER stress genes *CHOP* and *TRB3*, and XBP1 mRNA splicing, which can lead to apoptosis (Yokouchi et al., 2008). In addition, oxidative stress can down-regulate the level of the antiapoptotic protein survivin (Zhang et al., 2008) and may disrupt mitochondrial membrane potential, leading to the release of cytochrome *c*. Finally, oxidative stress may also result in DNA, RNA, or protein damage (Pan et al., 2005).

Our studies demonstrate for the first time that the NF-κB inhibitor DHMEQ causes apoptosis in liver cancer cells through the induction of oxidative stress. We observed that DHMEQ induced, in a dose-dependent fashion, phosphorylation of ERK1/2 as a prosurvival response of cells to the oxidative stress induced by DHMEQ. The combination of the specific MEK inhibitor U0126 with DHMEQ significantly reduced cell growth. In the presence of NAC, ERK1/2 was not activated, indicating that this survival signal is a response to ROS generation. However, this is a futile attempt of the cells because the proapoptotic signaling pathways become predominant.

ER stress response is a major mechanism mediating apoptotic cell death. Our results elucidated the induction by DHMEQ of ER stress response and that this response is an event downstream of the oxidative stress in hepatoma cells. These results are in accordance with results from other authors, who reported that the ER stress response could be induced through ROS species generation (Tagawa et al., 2008). ER stress response starts with GRP78 mRNA induction, which is a survival signal (Li and Lee, 2006). We found GRP78 induction is triggered by DHMEQ only in HA22T/VGH cells. The absence of its induction in HuH-6 cells could explain the differential sensibility to DHMEQ between the two cell lines. The failure of the unfolded protein response to maintain cellular homeostasis promotes ER stress-apoptotic signaling. One candidate for the apoptotic pathway is *CHOP*, a gene induced by oxidative stress (Zinszner et al., 1998). CHOP has been reported to be a positive transactivator of other inducible ER stress genes, such as *TRB3* (Ohoka et al., 2005). Accordingly, our results demonstrated that DHMEQ promotes CHOP and TRB3 mRNA induction and splicing of XBP1 mRNA in a ROS-dependent manner in hepatoma cells, and knockdown of TRB3 in HA22T/VGH cells significantly reverted DHMEQ-induced cell growth inhibition.

Ir remains unclear how ROS generate ER stress response. Previous reports demonstrated that ROS cause inhibition of a Ca^{2+}-ATPase and induced depletion of calcium stores in the ER, thereby resulting in ER stress (Moreau et al., 1998). However, our results demonstrated that neither BAPTA-AM nor EGTA reverted DHMEQ-induced cell growth inhibition. Furthermore, dantrolene, which inhibits Ca^{2+} release from the sarcoplasmic reticulum, also did not revert DHMEQ-induced cell growth inhibition. These results indicate that DHMEQ induced ER stress in a Ca^{2+}-independent mechanism.

Recent reports point to mitochondria as a critical apoptotic checkpoint at which converge ROS generation and ER stress response (Ni et al., 2008; Pinton et al., 2008). Our results point to mitochondrial generation of ROS induced by DHMEQ. Moreover, we demonstrated that DHMEQ induced the activation of caspase 8 in a ROS-dependent fashion. It has been reported that the caspase-8 pathway induced the ER stress response and that this was associated with release of cytochrome *c* from mitochondria in human hepatoma cells (Iizaka et al., 2007). Our results demonstrated that DHMEQ promoted the release of cytochrome *c* and of Prdx-3 in the cytosol, which depends on ROS production. Release of cytochrome *c* into cytosol causes activation of caspase cascades. Consequently, in this study, we observed the activation of caspases-3/7 and -9, and the cleavage of PARP, a well known caspase-3 target, which were triggered by DHMEQ in a ROS-dependent manner. Therefore, our data link ROS generation with mitochondrial apoptotic pathway and caspase activation as reported by others (Meeran et al., 2008; Ni et al., 2008). Moreover, the levels of survivin, an antiapoptotic protein member of the inhibitor of apoptosis (IAP) family, were reduced by DHMEQ treatment, and this was dependent on ROS production, as reported in other cancer cells (Zhang et al., 2008).

Finally, ROS have multiple effects on intracellular targets. In fact, they can damage DNA, RNA, and protein. We observed that DHMEQ treatment in hepatoma cells resulted in ROS-mediated DNA damage as increase levels of γ-H2AX were detected.

In summary, our results indicate that the main signal responsible for DHMEQ antitumor effects in human hepatoma cells is ROS production. Our findings on DHMEQ as an inducer of ROS highlight the potential of oxidative stress inducers as novel therapeutic drugs for liver cancer treatment.

Acknowledgments. We thank Dr. Andreina Bruno of Institute of Biomedicine and Molecular immunology "Alberto Monroy," C.N.R., for her assistance in the measurement of ROS production by flow cytometry analysis.

References

Ariga A, Namekawa J, Matsumoto N, Inoue J, and Umezawa K (2002) Inhibition of tumor necrosis factor-alpha -induced nuclear translocation and activation of NF-kappa B by dehydroxymethylepoxyquinomicin. *J Biol Chem* **277:**24625–24630.

Bowie A and O'Neill LA (2000) Oxidative stress and nuclear factor-kappaB activation: a reassessment of the evidence in the light of recent discoveries. *Biochem Pharmacol* **59:**13–23.

Buccellato LJ, Tso M, Akinci OI, Chandel NS, and Budinger GR (2004) Reactive oxygen species are required for hyperoxia-induced Bax activation and cell death in alveolar epithelial cells. *J Biol Chem* **279:**6753–6760.

Cabello CM, Bair WB 3rd, and Wondrak GT (2007) Experimental therapeutics: targeting the redox Achilles heel of cancer. *Curr Opin Investig Drugs* **8:**1022–1037.

Cervello M, Giannitrapani L, Labbozzetta M, Notarbartolo M, D'Alessandro N, Lampiasi N, Azzolina A, and Montalto G (2004a) Expression of WISPs and of their novel alternative variants in human hepatocellular carcinoma cells. *Ann N Y Acad Sci* **1028**:432–439.

Cervello M, Giannitrapani L, La Rosa M, Notarbartolo M, Labbozzetta M, Poma P, Montalto G, and D'Alessandro N (2004b) Induction of apoptosis by the proteasome

inhibitor MG132 in human HCC cells: possible correlation with specific caspase-dependent cleavage of beta-catenin and inhibition of beta-catenin-mediated transactivation. Int J Mol Med **13:**741–748.
Chen CY, Chen CH, Lo YC, Wu BN, Wang HM, Lo WL, Yen CM, and Lin RJ (2008) Anticancer activity of isoobtusilactone from *Cinnamomum kotoense*: involvement of apoptosis, cell-cycle dysregulation, mitochondria regulation, and reactive oxygen species. *J Nat Prod* **71:**933–940.
Chen Y, McMillan-Ward E, Kong J, Israels SJ, and Gibson SB (2007) Mitochondrial electron-transport-chain inhibitors of complexes I and II induce autophagic cell death mediated by reactive oxygen species. *J Cell Sci* **120:**4155–4166.
Choi SE, Kim HE, Shin HC, Jang HJ, Lee KW, Kim Y, Kang SS, Chun J, and Kang Y (2007) Involvement of Ca^{2+}-mediated apoptotic signals in palmitate-induced MIN6N8 beta cell death. *Mol Cell Endocrinol* **272:**50–62.
Danial NN and Korsmeyer SJ (2004) Cell death: critical control points. *Cell* **116:** 205–219.
Fang J, Nakamura H, and Iyer AK (2007) Tumor-targeted induction of oxystress for cancer therapy. *J Drug Target* **15:**475–486.
Gupta A, Rosenberger SF, and Bowden GT (1999) Increased ROS levels contribute to elevated transcription factor and MAP kinase activities in malignantly progressed mouse keratinocyte cell lines. *Carcinogenesis* **20:**2063–2073.
Haidara K, Marion M, Gascon-Barré M, Denizeau F, and Averill-Bates DA (2008) Implication of caspases and subcellular compartments in tert-butylhydroperoxide induced apoptosis. *Toxicol Appl Pharmacol* **229:**65–76.
Henderson LM, Chappell JB, and Jones OT (1989) Superoxide generation is inhibited by phospholipase A_2 inhibitors. Role for phospholipase A_2 in the activation of the NADPH oxidase. *Biochem J* **264:**249–255.
Iizaka T, Tsuji M, Oyamada H, Morio Y, and Oguchi K (2007) Interaction between caspase-8 activation and endoplasmic reticulum stress in glycochenodeoxycholic acid-induced apoptotic HepG2 cells. *Toxicology* **241:**146–156.
Kuznetsov AV, Smigelskaite J, Doblander C, Janakiraman M, Hermann M, Wurm M, Scheidl SF, Sucher R, Deutschmann A, and Troppmair J (2008) Survival signaling by C-RAF: mitochondrial reactive oxygen species and Ca^{2+} are critical targets. *Mol Cell Biol* **28:**2304–2313.
Lee AH, Iwakoshi NN, and Glimcher LH (2003) XBP-1 regulates a subset of endoplasmic reticulum resident chaperone genes in the unfolded protein response. *Mol Cell Biol* **23:**7448–7459.
Li J and Lee AS (2006) Stress induction of GRP78/BiP and its role in cancer. *Curr Mol Med* **6:**45–54.
Liu P, Kimmoun E, Legrand A, Sauvanet A, Degott C, Lardeux B, and Bernuau D (2002) Activation of NF-kappa B, AP-1 and STAT transcription factors is a frequent and early event in human hepatocellular carcinomas. *J Hepatol* **37:**63–71.
Matsukawa J, Matsuzawa A, Takeda K, and Ichijo H (2004) The ASK1-MAP kinase cascades in mammalian stress response. *J Biochem* **136:**261–265.
McCord JM (1985) Oxygen-derived free radicals in postischemic tissue injury. *N Engl J Med* **312:**159–163.
Meeran SM, Katiyar S, and Katiyar SK (2008) Berberine-induced apoptosis in human prostate cancer cells is initiated by reactive oxygen species generation. *Toxicol Appl Pharmacol* **229:**33–43.
Moreau VH, Castilho RF, Ferreira ST, and Carvalho-Alves PC (1998) Oxidative damage to sarcoplasmic reticulum Ca^{2+}-ATPase AT submicromolar iron concentrations: evidence for metal-catalyzed oxidation. *Free Radic Biol Med* **25:**554–560.
Ni Y, Gong XG, Lu M, Chen HM, and Wang Y (2008) Mitochondrial ROS burst as an early sign in sarsasapogenin-induced apoptosis in HepG2 cells. *Cell Biol Int* **32:**337–343.
Nishimura D, Ishikawa H, Matsumoto K, Shibata H, Motoyoshi Y, Fukuta M, Kawashimo H, Goto T, Taura N, Ichikawa T, et al. (2006) DHMEQ, a novel NF-kappaB inhibitor, induces apoptosis and cell-cycle arrest in human hepatoma cells. *Int J Oncol* **29:**713–719.
Nonn L, Berggren M, and Powis G (2003) Increased expression of mitochondrial peroxiredoxin-3 (thioredoxin peroxidase-2) protects cancer cells against hypoxia and drug-induced hydrogen peroxide-dependent apoptosis. *Mol Cancer Res* **1:**682–689.
Ohoka N, Yoshii S, Hattori T, Onozaki K, and Hayashi H (2005) TRB3, a novel ER stress-inducible gene, is induced via ATF4–CHOP pathway and is involved in cell death. *EMBO J* **24:**1243–1255.
Oyadomari S and Mori M (2004) Roles of CHOP/GADD153 in endoplasmic reticulum stress. *Cell Death Differ* **11:**381–389.
Pan J, She M, Xu ZX, Sun L, and Yeung SC (2005) Farnesyltransferase inhibitors induce DNA damage via reactive oxygen species in human cancer cells. *Cancer Res* **65:**3671–3681.
Pinton P, Giorgi C, Siviero R, Zecchini E, and Rizzuto R (2008) Calcium and apoptosis: ER-mitochondria Ca^{2+} transfer in the control of apoptosis. *Oncogene* **27:**6407–6418.
Poma P, Notarbartolo M, Labbozzetta M, Sanguedolce R, Alaimo A, Carina V, Maurici A, Cusimano A, Cervello M, and D'Alessandro N (2006) Antitumor effects of the novel NF-kappaB inhibitor dehydroxymethyl-epoxyquinomicin on human hepatic cancer cells: analysis of synergy with cisplatin and of possible correlation with inhibition of pro-survival genes and IL-6 production. *Int J Oncol* **28:**923–930.
Richter C and Schweizer M (1997) Oxidative stress and the molecular biology of antioxidant defences (Scandalios JG ed), Cold Spring Harbor Laboratory Press, Plainview, NY.
Riganti C, Costamagna C, Bosia A, and Ghigo D (2006) The NADPH oxidase inhibitor apocynin (acetovanillone) induces oxidative stress. *Toxicol Appl Pharmacol* **212:**179–187.
Starenki DV, Namba H, Saenko VA, Ohtsuru A, Maeda S, Umezawa K, and Yamashita S (2004) Induction of thyroid cancer cell apoptosis by a novel nuclear factor kappaB inhibitor, dehydroxymethylepoxyquinomicin. *Clin Cancer Res* **10:** 6821–6829.
Suzuki Y, Sugiyama C, Ohno O, and Umezawa K (2004) Preparation and biological activities of optically active dehydroxymethylepoxyquinomicin, a novel NF-kB inhibitor. *Tetrahedron* **60:**7061–7066.
Suzuki E, Sugiyama C, and Umezawa K (2009) Inhibition of inflammatory mediator secretion by (−)-DHMEQ in mouse bone marrow-derived macrophages. *Biomed Pharmacother* **63:**351–358.
Szatrowski TP and Nathan CF (1991) Production of large amounts of hydrogen peroxide by human tumor cells. *Cancer Res* **51:**794–798.
Tagawa Y, Hiramatsu N, Kasai A, Hayakawa K, Okamura M, Yao J, and Kitamura M (2008) Induction of apoptosis by cigarette smoke via ROS-dependent endoplasmic reticulum stress and CCAAT/enhancer-binding protein-homologous protein (CHOP). *Free Rad Biol Med* **45:**50–59.
Trudel S, Pâquet MR, and Grinstein S (1991) Mechanism of vanadate-induced activation of tyrosine phosphorylation and of the respiratory burst in HL60 cells. Role of reduced oxygen metabolites. *Biochem J* **276:**611–619.
Ueda S, Masutani H, Nakamura H, Tanaka T, Ueno M, and Yodoi J (2002) Redox control of cell death. *Antioxid Redox Signal* **4:**405–414.
Umezawa K and Chaicharoenpong C (2002) Molecular design and biological activities of NF-kappaB inhibitors. *Mol Cells* **14:**163–167.
Umezawa K (2006) Inhibition of tumor growth by NF-kappaB inhibitors. *Cancer Sci* **97:**990–995.
von Harsdorf R, Li PF, and Dietz R (1999) Signaling pathways in reactive oxygen species-induced cardiomyocyte apoptosis. *Circulation* **99:**2934–2941.
Yokouchi M, Hiramatsu N, Hayakawa K, Okamura M, Du S, Kasai A, Takano Y, Shitamura A, Shimada T, Yao J, et al. (2008) Involvement of selective oxygen species upstream of preapoptotic branches of unfolded protein response. *J Biol Chem* **283:**4252–4360.
Zhang R, Humphreys I, Sahu RP, Shi Y, and Srivastava SK (2008) In vitro and in vivo induction of apoptosis by capsaicin in pancreatic cancer cells is mediated through ROS generation and mitochondrial death pathway. *Apoptosis* **13:**1465–1478.
Zinszner H, Kuroda M, Wang X, Batchvarova N, Lightfoot RT, Remotti H, Stevens JL, and Ron D (1998) CHOP is implicated in programmed cell death in response to impaired function of the endoplasmic reticulum. *Genes Dev* **12:**982–995.

Address correspondence to: Nadia Lampiasi, Istituto di Biomedicina e Immunologia Molecolare "Alberto Monroy," (C.N.R.), Via Ugo La Malfa 153, 90146 Palermo, Italy. E-mail: lampiasi@ibim.cnr.it